EPSC Abstracts
Vol. 13, EPSC-DPS2019-58-1, 2019
EPSC-DPS Joint Meeting 2019

EPSC
EPSC-DPS Joint Meeting 2019
15–20 September 2019 | Geneva, Switzerland

New Results on Mars Mesospheric CO_2 Ice Clouds from the Mars Reconnaissance Orbiter (MRO)

Todd Clancy (1), Mike Wolff (1), Mike Smith (2), Armin Kleinböhl (3), and Bruce Cantor (4)
(1) Space Science Institute, Colorado, USA, (2) NASA/GSFC, Maryland, USA, (3) JPL/Caltech, California, USA, (4) Malin Space Science Systems, California, USA, (clancy@spacescience.org).

Abstract

An analysis of 2009-2016 MRO CRISM visible/near-IR (λ = 0.4-4 μm) limb spectra defines the spatial and orbital/seasonal distributions (consistent with earlier studies) of daytime (3pm) mesospheric (altitudes of 55-75 km) CO_2 ice clouds, including their particle sizes (R_{eff} =0.3-2.5μm) and size distribution variances (ν_{eff} =0.03, indicative of iridescence) [1]. The analysis emphasizes single scattering comparisons generated from T-matrix phase function calculations [2] for equidimensional disk shapes (D/L=1), although a subset of full multiple scattering, profile retrievals are employed for comparison. These CRISM-derived properties are compared to near-coincident MRO MCS thermal-IR limb scattered radiances from mesospheric CO_2 clouds. The MCS limb radiances also indicate, for the first time, nighttime CO_2 clouds (3am) with larger particle sizes (R_{eff} ~7μm) at 55-60 km altitudes [1]. Coincident MRO MARCI wide-angle imaging further demonstrates the large horizontal extent of the daytime observed CO_2 ice clouds, including their wave/cirrus morphologies [1].

1. CRISM

Roughly 1100 CRISM limb profile observations were obtained over MY29-33, with full (5-10º spacing) latitudinal coverage, limited longitude sampling (~0W, 70W, 105W, and 300 W), and good seasonal/orbital (solar longitude, L_s = 35-360º) coverage (although irregularly spaced among the 4 MYs sampled).

The broad CRISM spectral dependence of observed CO_2 ice cloud scattering defines its composition and particle size, whereas spectral interference 'waves' in their spectra indicate iridescence associated with very narrow size distributions (ν_{eff} = 0.03), which likely applies for all particle size, CO_2 cloud populations (R_{eff} =0.3-2.5μm) observed (see figure 1). Such narrow particle size distributions indicate uniform particle growth histories within individual mesospheric CO_2 clouds, suggesting abrupt cloud formation and uniform cloud nucleation centers, such as perhaps provided by meteoritic ion chemistry [3]. This is the first measurement of cloud iridescence in a planetary atmosphere other than the Earth, where such behavior is infrequently observed. Iridescent displays are a feature of smaller (R_{eff} <5-10μm) ice particle sizes [4] not typically presented in the terrestrial atmosphere, except at high altitudes or in jet contrails.

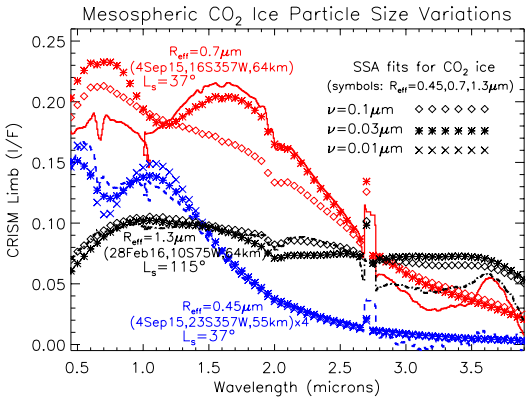

Figure 1: A set of CRISM limb spectra of scattering by mesospheric CO_2 clouds of various particle sizes (lines; R_{eff} =1.3μm-black, 0.7μm-red, 0.45μm-blue). Models for the above R_{eff} are presented for three distinct size distribution variances (symbols; ν_{eff} = 0.1-diamonds, 0.03-asterisks, 0.01-X's). The narrower size distributions present iridescence in the smaller particle size cases (red and blue) as interference patterns in the reflectance spectra.

The global Mars atmosphere exhibits strong orbital variations in temperature, photochemistry (associated with condensation-forced water vapor variation), and aerosol behaviors [5]. This behavior reflects the large eccentricity of the Mars orbit (e ~0.09). The orbital aerosol variations in the mesosphere are distinct from those exhibited in the lower atmosphere (such as the aphelion cloud belt and perihelion dust storms). Figure 2 presents this orbital dichotomy in mesospheric aerosols as revealed in the CRISM limb aerosol analysis.

To first order, CO_2 ice clouds dominate aerosols in the aphelion mesosphere (yellow/white symbols in the top panel of figure 2), and water ice clouds (green/blue symbols) and dust (red symbols) dominate aerosol behavior in the perihelion mesosphere (lower panel of figure 2). Dust aerosols were infrequently observed in the non-global dust years of the CRISM limb observations [1], but are prominent during planet encircling dust storms [6,7]. The aphelion correspondence with CO_2 clouds reflects the much colder (and drier) conditions associated with 40% reduced solar heating relative to perihelion. The top panel of figure 2 presents the latitude/altitude distribution of mesospheric CO_2 clouds measured by CRISM, where smaller cloud particle sizes (R_{eff} <1 μm) occur at the latitude/altitude margins of the large particle size (R_{eff} >1 μm) cloud region.

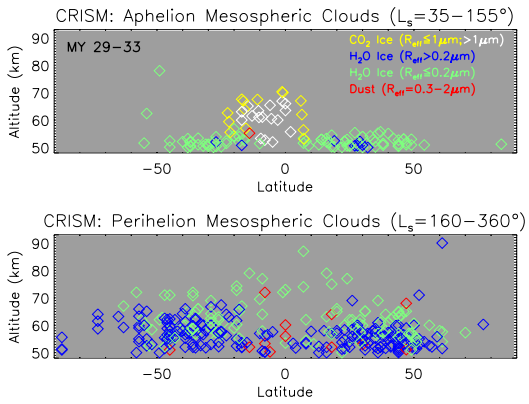

Figure 2. Altitude/latitude cross sections of the accumulated distributions for 2009-2016 CRISM analyzed particle sizes and compositions for discrete mesospheric aerosol layers, as observed over aphelion (upper) and perihelion (lower) portions of the Mars year. Aerosol composition (yellow/white- CO_2 ice, blue/green- H_2O ice, red- dust) and particle size (yellow vs. white, green vs. blue, as on figure) are indicated by color.

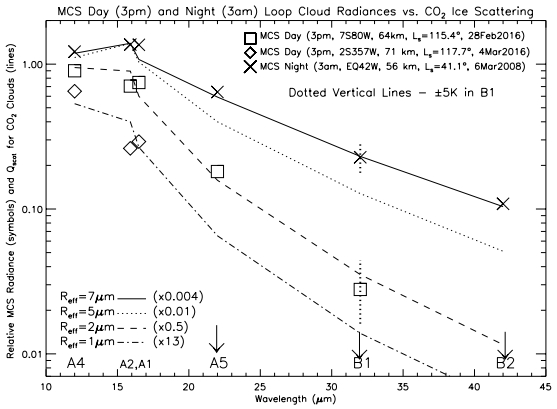

Figure 3: Scaled MCS channel radiances (diamonds and squares-3pm, X's-3am) are compared to CO_2 ice scattering efficiencies for R_{eff} =1-7 μm particle sizes.

The latitudinal (20S-10N), longitudinal (0W and 70W), altitude (55-70 km), and L_s distributions of mesospheric CO_2 clouds observed in CRISM limb spectra reflect cold aphelion conditions, but also minimum temperature regions associated with Mars atmospheric tides and gravity waves. These CO_2 cloud spatial/temporal distributions generally agree with results of prior studies for these clouds [8-12]. The orbital dichotomy between CO_2 versus H_2O cloud occurrence and the particle size spatial/temporal variations of figure 2 are new results.

2. MCS

MCS measure vertical profiles of 11-45μm thermal IR radiance for retrieval Mars atmospheric temperature, dust, and H_2O ice profiles with high vertical and latitudinal sampling rates [13]. Although CO_2 ice is not a standard retrieval product, MCS is sensitive to scattering by CO_2 ice clouds [14,15] and provides near-coincident comparisons with CRISM CO_2 cloud measurements, including particle size sensitivity. Figure 3 presents two such daytime (diamond and squares symbols, 3pm) MCS detections of conservative scattering by mesospheric CO_2 clouds of surface thermal-IR radiance, corresponding to near-coincident CRISM cloud detections. Relative MCS radiances are plotted versus MCS IR wavelength (and indicated channel) for comparison to the wavelength-dependent scattering cross sections for CO_2 ice particle R_{eff} of 1 and 2 μm, reasonably consistent with the CRISM particle size determinations [1].

More surprisingly, MCS nighttime (X symbols, 3am) scattering by CO_2 clouds 5-10km lower in altitude indicate much large particle sizes (R_{eff} ~7 μm). These nighttime lower mesospheric CO_2 clouds are distinct from nighttime CO_2 fine ice hazes detected at ~100 km altitudes in stellar occultations [16], although thermal tides and gravity waves likely play key roles the formation of all of these mesospheric CO_2 ice aerosols. However, MCS observations indicate that these nighttime lower mesospheric CO_2 clouds are among the brightest, largest particle size, and most pervasive (e.g., figures 6C and 7C of [17]) of all such mesospheric CO_2 ice cloud occurrences [1].

3. MARCI

Wide angle color imaging from MARCI provides coincident nadir imaging of the horizontal (latitude and longitude) extent and morphology (at ~1 km spatial resolution) of mesospheric CO_2 clouds incorporated in the CRISM limb field of view (fov). Figure 4 presents MARCI color (RGB, left) and violet (437nm, right), images of a large expanse (~500km x 500km) of mesospheric CO_2 cloud forms corresponding to CRISM limb spectral measurements of bright CO_2 clouds over 17S to the equator (with R_{eff} ranging from 0.8-2.2 μm). The CRISM fov is in the plane of the MRO polar orbit, 1-2º left of center in the MARCI images. The color MARCI image map (left)

reflects registration of the individual RGB filter images (staggered in orbit plane) to the Mars surface, such that the mesospheric cloud colors are improperly overlain. Registration of the image to a 70 km altitude (as indicated in the CRISM limb data for these clouds) leads to proper color registration for the clouds. The right image map presents the violet image map registered to this altitude, to display the wave form and zonal orientation of these mesospheric clouds.

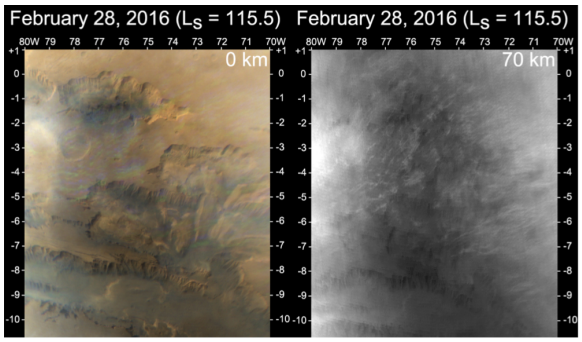

Figure 4: MARCI color (left) and violet (right) image maps display a regional-scale outbreak of mesospheric CO_2 clouds over Valles Marineris. The ~70 km cloud altitudes lead to their color misalignment in the surface-registered RGB image. They are registered at 70 km altitude in the violet (437nm) image.

Only very bright mesospheric clouds, over regions of reduced lower atmospheric clouds (which are H_2O ice) for maximum contrast, allow optimum MARCI nadir imaging of mesospheric clouds. Higher spatial resolution nadir imaging of mesospheric CO_2 clouds have been obtained from OMEGA [9, 10], THEMIS [11], CRISM [12], and HRSC [18]. MARCI wide-angle imaging demonstrates that mesospheric CO_2 ice clouds exist over regional scales, and so require that the gravity wave forcing postulated to create very cold regions (T<110K) sufficient for CO_2 condensation [19-22] must also be present on such large scales.

Further information

A much broader range of mesospheric aerosol results associated with CRISM limb spectra and CRISM-MCS-MARCI comparisons is presented in [1], including mesospheric H_2O ice and dust aerosols and additional results regarding mesospheric CO_2 clouds.

Acknowledgements

We are indebted to the MRO and CRISM operations staff for the collection and processing of CRISM limb observations. Grant support for this work was provided by the NASA MDAP Program (under NASA contract award number NNX15AQ07G). Additionally, parts of this work were performed at the Jet Propulsion Laboratory, California Institute of Technology, under a contract with the National Aeronautics and Space Administration.

References

[1] Clancy, R.T., Wolff, M., Smith, M., Kleinböhl, A., Cantor, B., Murchie, S., Toigo, A., Seelos, K., Lefèvre, F., Montmessin, F., Daerden, F., and Sandor, B.: The distribution, composition, and particle properties of Mars mesospheric aerosols: An analysis of CRISM visible/near-IR limb spectra with context from near-coincident MCS and MARCI observations, Icarus, 328, 246-273, 2019.

[2] Mishchenko, M., Travis, L., and Macke, A.: Scattering of light by polydiverse randomly oriented, finite circular cylinders, Applied Optics, 35, 4927-4940, 1996.

[3] Plane, J., Carrillo-Sanchez, J., Mangan, T., Crismani, M., Schneider, N., and Määttänen, A.: Meteoric chemistry in the Martian atmosphere, J. Geophys. Res., 123, 695-707, 2018.

[4] Haberle, R., Clancy, T., Forget, F., Smith, M., and Zurek, R., eds.: The Atmosphere and Climate of Mars, Cambridge University Press, 2017.

[5] Sassen, K.: Cirrus cloud iridescence: A rare case study, Applied Optics, 42, 486-491, 2003.

[6] Clancy, T., Wolff, M., Whitney, B., Cantor, B., Smith, M., McConnochie, T.: Extension of atmospheric dust loading to high altitudes during the 2001 Mars dust storm: MGS TES limb observations, Icarus, 207, 98-109, 2010.

[7] Määttänen, A., Listowski, C., Montmessin, F., Maltagliati, L., Reberac, A., Joly, L., and Bertaux, J.-L.,: A complete climatology of the aerosol vertical distribution on Mars from Mex/SPICAM UV solar occultations, Icarus, 223, 892-941, 2013.

[8] Clancy, T., Wolff, M., Whitney, B., Cantor, B., and Smith, M.: Mars equatorial mesospheric clouds: Global occurrence and physical properties from Mars Global Surveyor Thermal Emission Spectrometer and Mars Orbiter Camera limb observations, J. Geophys. Res., 112, 1-18, 2007.

[9] Montmessin, F., Gondet, B., Bibring, J.-P., Langevin, Y., Drossart, P., Forget, F., and Fouchet, T.: Hyperspectral imaging of convective CO_2 ice clouds in the equatorial mesosphere of Mars, J. Geophys. Res., 112, 1-14, 2007.

[10] Määttänen, A., Montmessin, F., Gondet, B., Scholten, F., Hoffmann, H., González-Galindo, F., Spiga, A., Forget, F., Hauber, E., Neukum, G., Bibring, J.-L., and Bertaux, J.-L.: Mapping the mesospheric CO_2 clouds on Mars: Mex/OMEGA and Mex/HRSC observations and challenges for atmospheric models, Icarus, 209, 452-469, 2010.

[11] McConnochie, T., Bell III, J., Savransky, D., Wolff, M., Toigo, A., Wang, W., Richardson, M., and Christensen, P.: THEMIS-VIS observations of clouds in the martian mesosphere: Altitudes, wind speeds, and decameter-scale morphology, Icarus, 210, 545-565, 2010.

[12] Vincendon, M., Pilorget, C., Gondet, B., Murchie, S., and Bibring, J.-P.: New near-IR observations of mesospheric CO_2 and H_2O clouds on Mars, J. Geophys. Res., 116, 1-18, 2011.

[13] Kleinböhl, A., Schofield, T., Kass, D., Abdou, W., Backus, C., Sen, B., Shirley, J., Lawson, G., Richardson, M., Taylor, F., Teanby, N., and McCleese, D.: Mars Climate Sounder limb profile retrieval of atmospheric temperature, pressure, and dust and water ice opacity, J. Geopyhs. Res., 114, 1-30, 2009.

[14] Hayne, P., Paige, D., Schofield, T., Kass, D., Kleinböhl, A., Heavens, N., and McCleese, D.: Carbon dioxide snow clouds on Mars: South polar winter observations by the Mars Climate Sounder, J. Geophys. Res., 117, 1-23, 2012.

[15] Puspitarini, L., Määttänen, A., Fouchet, T., Kleinböhl, A., Kass, D., and Schofield, T., Analysis of high altitude clouds in the Martian atmosphere based on Mars Climate Sounder observations, J. Phys. Conf. Ser., 771, 1-4, 2016

[16] Montmessin, F., Bertaux, J.-L., Quémerais, E., Korablev, O., Rannou, P., Forget, F., Perrier, S., Fussen, D., Lebonnois, S., Rébérac, A., and Dimarellis, E.: Subvisible CO_2 ice clouds detected in the mesosphere of Mars, Icarus, 183, 403-410, 2006.

[17] Sefton-Nash, E., Teanby, N., Montabone, L., Irwin, P., Hurley, J., and Calcutt, S.: Climatology and first-order composition estimates of mesospheric clouds from Mars Climate Sounder limb spectra, Icarus, 222, 342-365, 2013.

[18] Scholten, F., Hoffman, H., Määttänen, A., Montmessin, F., Gondet, B., and Hauber, E.: Concatenation of HRSC colour and OMEGA data for the determination and 3D-parameterization of high-altitude CO_2 clouds in the Martian atmosphere, Planetary Space Sci., 58, 1207-1214, 2010.

[19] Clancy, T., and Sandor, B.: CO_2 ice clouds in the upper atmosphere of Mars, Geophys. Res., 25, 489-492, 1998.

[20] Spiga, A., González-Galindo, F., López-Valverde, M., and Forget, F.: Gravity waves, cold pockets and CO2 clouds in the Martian mesosphere, Geophys. Res. Lett., 39, 1-5, 2012.

[21] Listowski, C., Määttänen, A., Montmessin, F., Spiga, A., and Lefèvre, F.: Modeling the microphysics of CO2 ice clouds within the wave-induced cold pockets in the Martian mesosphere, Icarus, 237, 239-261, 2014.

[22] Yigit, E., Medvedev, A., and Hartogh, P.: Gravity waves and high-altitude CO_2 ice cloud formation in the Martian atmosphere, Geophys. Res. Lett., 42, 4294-4300, 2015.